



Supernova Remnants in Gamma Rays

Andrea Giuliani ^{1,*}  and Martina Cardillo ² ¹ INAF—Istituto di Astrofisica Spaziale e Fisica Cosmica, Via Alfonso Corti 12, 20133 Milano, Italy² INAF—Istituto di Astrofisica e Planetologia Spaziali, Via del Fosso del Cavaliere 100, 00133 Roma, Italy; martina.cardillo@inaf.it

* Correspondence: andrea.giuliani@inaf.it

Abstract: In the 1960s, the remnants of supernova explosions (SNRs) were indicated as a possible source of galactic cosmic rays through the Diffusive Shock Acceleration (DSA) mechanism. Since then, the observation of gamma-ray emission from relativistic ions in these objects has been one of the main goals of high-energy astrophysics. A few dozen SNRs have been detected at GeV and TeV photon energies in the last two decades. However, these observations have shown a complex phenomenology that is not easy to reduce to the standard paradigm based on DSA acceleration. Although the understanding of these objects has greatly increased, and their nature as efficient electron and proton accelerators has been observed, it remains to be clarified whether these objects are the main contributors to galactic cosmic rays. Here, we review the observations of γ -ray emission from SNRs and the perspectives for the future.

Keywords: supernova remnants; high energy; PeVatrons; galactic cosmic rays

1. Supernova Remnants

1.1. Supernova Remnant Evolution

Supernova explosions can result from two main physical processes related to the life cycle of a star. The first one happens when a star with a mass greater than $8 M_{\odot}$ reaches the end of its life, and the radiation produced within the nucleus is no longer able to counteract the weight of the star's envelope. The collapse of the star triggers the material to produce a supernova explosion. Alternatively, a white dwarf in a binary system can exceed the Chandrasekhar equilibrium limit (approximately $1.4 M_{\odot}$) due to accretion from its companions and explode in a type Ia supernova. In both cases, the supernova explosion expels a significant amount of matter, ranging from 1 to several solar masses, into the interstellar medium at a speed of 10^4 km s^{-1} . This corresponds to a kinetic energy of approximately 10^{51} erg . The main differences between the two scenarios concern the chemical composition of the ejected materials and the interstellar medium (ISM) into which the supernova remnant (SNR) expands.

Over the subsequent 100,000 years, the ejecta will expand, interact with the surrounding medium, and eventually dissolve into it. The evolutionary phases of an SNR can be defined by the type of interaction with the surrounding medium and the ratio between the ejecta mass (M_{ej}) and the mass of the swept-up material (M_{sw}).

During the free expansion phase, lasting a few hundred years as long as $M_{\text{ej}} > M_{\text{sw}}$, the star's ejecta expands freely into the surrounding medium with an expansion law linear in time, $R \sim t$. In this phase, the material's speed exceeds the speed of sound in the surrounding medium, thus creating a shock. The temperature decreases as the gas expands adiabatically: $T \sim -3(\gamma - 1)$, where γ is the specific heat ratio.

In the Sedov–Taylor phase, lasting between 20,000 and 40,000 years as long as $M_{\text{ej}} \leq M_{\text{sw}}$, the deceleration of the shell becomes significant, and a reverse shock begins to propagate toward the interior of the SNR, heating the gas, which thus becomes



Citation: Giuliani, A.; Cardillo, M. Supernova Remnants in Gamma Rays. *Universe* **2024**, *10*, 203. <https://doi.org/10.3390/universe10050203>

Academic Editor: Fridolin Weber

Received: 29 February 2024

Revised: 21 April 2024

Accepted: 25 April 2024

Published: 1 May 2024



Copyright: © 2024 by the authors. Licensee MDPI, Basel, Switzerland. This article is an open access article distributed under the terms and conditions of the Creative Commons Attribution (CC BY) license (<https://creativecommons.org/licenses/by/4.0/>).

visible in the soft X-ray band. The evolution of the remnant is well described by the adiabatic blast-wave solution of Taylor and Sedov [1], and the radius increases with time as $R \propto t^{2/5}$.

The forward and reverse shocks formed during the free expansion and Sedov–Taylor phases can accelerate particles (see Section 1.2). The observation of non-thermal radio and γ -ray emissions from SNRs with ages up to a few tens of thousands of years confirms this aspect.

In the radiative phase ($M_{ej} \ll M_{sw}$), the shell expands at a sub-thermal speed. After this phase, the remnant of the supernova dissolves and becomes part of the interstellar medium.

The duration of each phase of an SNR is determined by the interaction between the ejecta and the ISM, which, in turn, depends on the type of circumstellar medium in which the SNR is situated. On the other hand, supernova explosions play a crucial role in shaping the evolution of the ISM and galaxies by injecting a significant amount of energy and momentum and then influencing the process of star formation [2]. Figure 1 shows the young SNR Cas A as seen in the X-ray.

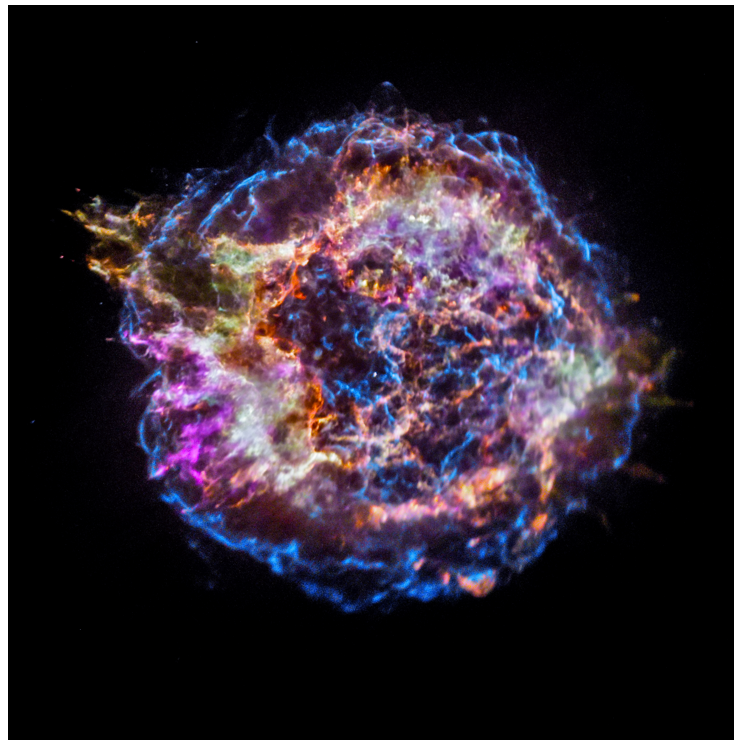


Figure 1. Cas A image in X-ray band as observed by the Chandra X-ray Observatory telescope [3].

1.2. Supernova Remnants as Cosmic Accelerators

In the initial two stages of an SNR's evolution, a shock forms between the ejecta (including swept material) and the local interstellar medium. Additionally, a second shock may develop and propagate toward the center.

Over the past decades, various works have shown how shocks can accelerate particles, including cosmic rays (CRs), and there is a consensus that the dominant process is Diffusive Shock Acceleration (DSA) [4,5]. This process is based on Fermi I-order acceleration [6]. The acceleration index provided by DSA, $\gamma = \frac{3R}{R-1}$, is strictly correlated with the compression ratio of the shock, $R = \frac{u_u}{u_d}$, where u_u and u_d are the upstream and downstream velocities, respectively, related to the shock Mach number. For strong shocks and in the test-particle limit, i.e., when the particle energy is negligible compared to that of the shock, DSA predicts a particle energy distribution with an energy spectral index close to 2. However, the backreaction of CRs on the shock and then also on the surrounding ambient can modify

the acceleration spectrum, and if the feedback effects on the shock are not negligible, the spectral index of accelerated particles may become steeper than 2 (for a review of the DSA theory, see [7] and references therein).

If SNRs accelerate cosmic rays (CRs), they should be observed as sources of non-thermal emission. This emission results from the interaction of electrons and hadrons with the surrounding medium. The interaction between electrons and magnetic fields at the site produces synchrotron radiation. If the electron spectral distribution can be described as a power law with index α and maximum energy E_{\max} (i.e., $f(E) \propto E^{-\alpha} \exp(E/E_{\max})$), the emerging emission has a spectrum with slope $\gamma = -(\alpha + 1)/2$, typically resulting in a hard spectrum. In the spectral energy distribution (SED, see Figure 2), the peak energy of synchrotron radiation can reach the X-ray band for an E_{\max} of few TeV. The same electron population interacting with the radiation fields produces emission through the Inverse Compton process. The emission has a spectral shape similar to that of the synchrotron but shifted toward higher energies, typically in the γ -ray band. If a dense medium is present, electrons can also radiate efficiently through Bremsstrahlung, which concurs with the γ -ray emission of the objects.

If hadrons (protons or heavier nuclei) are also accelerated, they scatter inelastically against the nuclei of the medium in the so-called “pp interaction”, producing neutral pions, which rapidly (8.5×10^{-17} s) decay into two γ -ray photons. In addition to protons, secondary electrons (produced by pp interactions) can produce γ -ray emission through IC and Bremsstrahlung (see [8] and references therein).

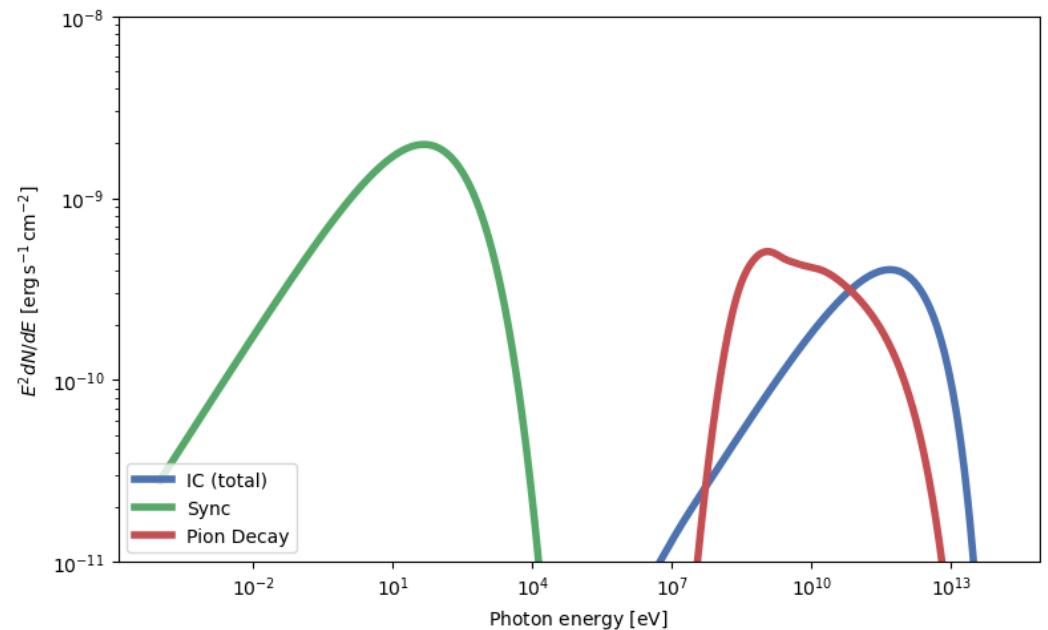


Figure 2. Example of SED given by synchrotron, IC and pion decay process.

SNRs have often been suggested as possible sources of CRs for two main reasons: their observed non-thermal emission (from radio to γ -ray) and a substantial match between the average power of supernova explosions in the Galaxy and the power needed to keep the galactic CR population stable. The energy density of CRs in the Galaxy disk is on the order of $w_{\text{CR}} \simeq 1 \text{ eV/cm}^3$. In the standard leaky-box approximation, we assume the disk of the Galaxy as a disk with a radius of 15 kpc and a height of 1 kpc, obtaining a total CR energy $E_{\text{CR}} = w_{\text{CR}} \times V_{\text{disk}} \simeq 3.34 \times 10^{55} \text{ erg}$. Isotope ratios in CRs can be used to estimate the typical permanence time of CRs in the plane of the Galaxy, which is approximately $t_{\text{disk}} \approx 10^7$ years. Therefore, assuming that the galactic CR distribution has reached a steady-state condition, the power needed to maintain the observed CR density is $P_{\text{CR}} = \frac{E_{\text{CR}}}{t_{\text{disk}}} \simeq 10^{41} \text{ erg/s}$. Whichever process accelerates CRs in the Galaxy, it must

therefore have a power of at least P_{CR} . A process with similar power is given by supernova explosions. Assuming that their average rate in our Galaxy is on the order of 1/30 years, we find that $P_{SN} \simeq 1 \simeq 10^{42}$ erg/s. The first to notice this similarity were Ginzburg and Syrovatskii [9], who concluded that “SuperNovae alone could maintain the CR population provided that about 10% of their kinetic energy is somehow converted into CRs”. This was the first evidence pointing to supernovae (or, equivalently, SNRs) as prime candidates for CR sources.

The observation of non-thermal emission from SNRs strongly supports the hypothesis that they could be sources of galactic CRs. Indeed, the synchrotron spectra of these objects have been observed in the radio band since the 1960s, showing the presence of magnetic field amplification [10–12], and the modification of Balmer lines in the optical band due to CR presence was also observed [13].

The majority of cosmic rays are hadrons. Therefore, evidence supporting the idea that supernova remnants can sustain the galactic cosmic-ray population must come from observations of these objects in the gamma-ray band. This is the only band where a clear indication of their presence can be found. Moreover, the cosmic-ray spectrum suggests that some galactic sources can accelerate particles to at least 1 PeV. This should result in a γ -ray spectrum up to and beyond 100 TeV, with no cutoffs.

For this reason, SNRs have always been a primary focus of γ -ray observations. This includes both the GeV band (approximately 0.1–100 GeV), which is covered by γ -ray satellites, and the TeV band (approximately 0.1–100 TeV), which is covered by Cherenkov telescopes. On the one hand, we now know that even the first γ -ray instruments (SAS-2, COS-B in the 1970s, EGRET on board CGRO in the 1990s) were able to detect these objects. On the other hand, the limited angular resolution of these instruments (and the crowding of the galactic fields) did not allow the γ -ray emission to be associated with SNRs.

The first certain associations were made with Cherenkov instruments; HEGRA observed a source associated with SNR W28, while H.E.S.S. was able to resolve the shell morphology of SNR RX J1713.7-3946 [14].

In recent years, many other classes of sources have been shown to accelerate CRs ([15] and reference therein), and consequently, it is crucial to understand whether the contribution of SNRs is dominant or not.

In this new context, another fundamental channel is neutrino detection. This is an unquestionable hint of CR acceleration since neutrinos can be produced only by the decay of charged pions produced by p-p and p- γ interactions [16]. Looking for neutrino detection in correspondence with PeVatron candidates can confirm the nature of γ -ray-emitting sources [17].

2. SNR in Gamma-Ray Band

Although an exhaustive classification of SNRs in γ -rays is not possible, certain groups of objects have been recognized over time based on their spectrum morphology and multiwavelength behavior [18] (a list of firmly identified SNRs in gamma-ray can be found in Table 1). In young (few thousand years) shell-like SNRs, the γ -ray emission comes from the shell, and often, there is a good morphological correlation between X-ray and γ -ray morphology. Some objects of this class are RX J1713.7-3946, RX J0852.0-4622, RCW 86, and SN 1006. They have similar γ -ray spectra, composed of a hard component (index < 2) peaking around a few TeV, followed by a rapid spectrum decrease. They also show similar γ -ray luminosities [19]. It has been proposed that this class of SNRs is leptonic; in this scenario, the SED can be modeled quite easily with a single electron population emitting in X-rays through a synchrotron and in γ -rays through IC [19]. However, other authors proposed hadronic models for at least some of these objects. For example, the spectrum of RXJ 1713.7-3946 can be explained in terms of hadronic emission, taking into account the clumpiness of the surrounding medium [20].

Another class of sources includes the SNRs interacting with molecular clouds (MCs). A list of SNRs in this class can be found in [21]. In these objects, the γ -rays originate

from a region of dense gas that is close to, or in contact with, the SNR. In these systems, typically, the target for the accelerating particles is the gas contained in large MCs (more than $10^3 M_{\odot}$). Some famous examples are W 44, W 28, IC 443, and W 51C. The γ -ray spectra of these objects have a soft index (>2.5) and are more easily observed in the GeV than in the TeV band. The ages of these SNRs reach several tens of thousands of years, and their γ -ray luminosities are $\geq 10^{35}$ erg/s. These spectra can be interpreted as γ -ray emissions from particles that diffuse in a partially ionized interstellar medium [22]. The interaction between the SNR shock and the MC can be observed through enhanced CO(2-1)/CO(1-0) ratios, OH maser emission at 1720 MHz, and SiO emission [23]. Additionally, this interaction can be traced using the neutral iron line induced by MeV protons in dense gas [24].

Notably, the very young SNRs Tycho and Cas A exhibit properties that are not easily classified within these two categories, with a spectral index that is intermediate between the two.

Table 1. List of SNRs firmly identified with a gamma-ray source. The Columns GeV, TeV, and PeV indicate detection, respectively, in the bands 0.1–100 GeV, 0.1–100 TeV, and >0.1 PeV.

Name	Common Name	GeV	TeV	PeV
G004.5+06.8	Kepler	Yes [25]	Yes [26]	-
G006.4-00.1	W28	Yes [27]	Yes [28]	-
G008.7-00.1	W30	Yes [29]	-	-
G020.0-00.2	-	Yes [30]	-	-
G023.3-00.3	W41	Yes [31]	Yes [31]	-
G024.7+00.6	-	Yes [30]	Yes [32]	-
G034.7-00.4	W44	Yes [33]	-	-
G043.3-00.2	W49B	Yes [34]	Yes [35]	-
G045.7-00.4	-	Yes [30]	-	-
G049.2-00.7	W51C	Yes [36]	Yes [37]	Yes [38]
G074.0-08.5	CygnusLoop	Yes [39]	-	-
G078.2+02.1	γ -Cygni	Yes [40]	Yes [41]	Yes [38]
G089.0+04.7	HB21	Yes [42]	-	-
G106.3+02.7	-	Yes [43]	Yes [44]	Yes [45]
G109.1-01.0	-	Yes [46]	-	-
G111.7-02.1	CasA	Yes [47]	Yes [48]	-
G120.1+01.4	Tycho	Yes [49]	Yes [50]	-
G132.7+01.3	HB3	Yes [51]	-	-
G160.9+02.6	HB9	Yes [52]	-	-
G180.0-01.7	S147	Yes [53]	-	-
G189.1+03.0	IC443	Yes [54]	Yes [55]	-
G205.5+00.5	Monoceros Loop	Yes [56]	-	-
G260.4-03.4	PuppisA	Yes [57]	-	-
G266.2-01.2	Vela Jr	Yes [58]	Yes [59]	-
G291.0-00.1	-	Yes [30]	-	-
G292.0+01.8	-	Yes [60]	-	-
G296.5+10.0	-	Yes [61]	-	-
G298.6-00.0	-	Yes [60]	-	-
G315.4-02.3	RCW86	Yes [62]	Yes [63]	-
G321.9-00.3	-	Yes [64]	-	-
G323.7-01.0	HESSJ1534-571	-	Yes [65]	-
G326.3-01.8	-	Yes [66]	-	-
G327.6+14.6	SN1006	Yes [67]	Yes [68]	-
G347.3-00.5	RXJ1713.7-3946	Yes [69]	Yes [70]	-
G348.5+00.1	CTB37A	Yes [71]	Yes [72]	-
G348.7+00.3	CTB37B	Yes [73]	Yes [74]	-
G349.7+00.2	-	Yes [75]	Yes [76]	-
G353.6-00.7	HESSJ1731-347	Yes [77]	Yes [78]	-
G355.4+00.7	-	Yes [30]	-	-
G357.7-00.1	MSH 17-39	Yes [79]	-	-

2.1. Cas A

Cas A is one of the youngest known SNRs in the Galaxy, with an estimated age of about 350 years. It is the remnant of a Type IIb supernova [80] that likely passed through a red supergiant phase [81]. The remnant is located at a distance of 3.4 ± 0.4 kpc [82].

In the γ -ray band, this SNR was extensively observed by Fermi-LAT [47], MAGIC [83], and Veritas [84], covering an energy range from 100 MeV to about 10 TeV (see Figure 3). A single-zone hadronic component can accurately model the GeV-TeV spectrum (see Figure 3). The population of protons is described by a power law with an index of 2.17 and a cutoff energy of 17 TeV [85]. However, the contribution of a leptonic component cannot be ruled out.

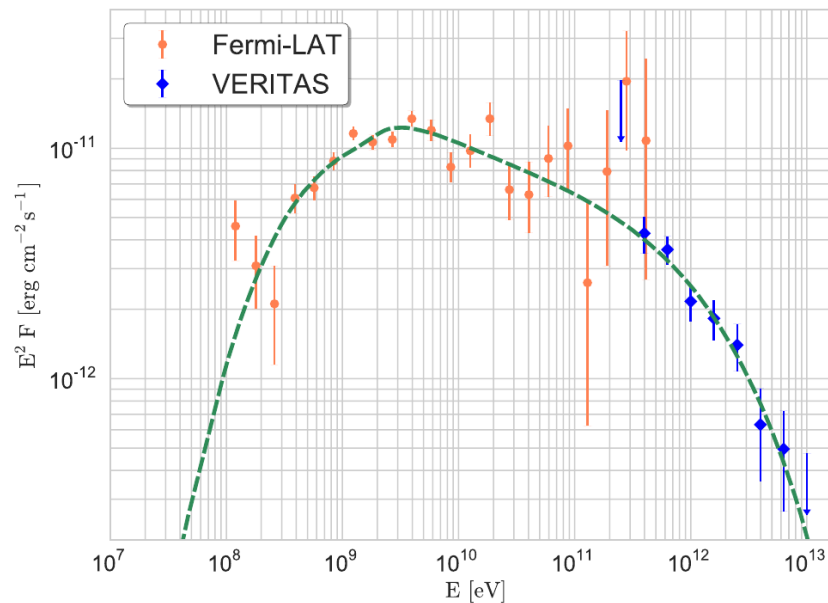


Figure 3. The Cas A spectrum, as seen by Fermi and Veritas (Figure from [85]). The dashed line represents a hadronic model for this source.

Given the observational evidence for a reverse shock in Cas A [86,87], a two-zone model with both forward and reverse shocks has been adopted for multiwavelength emission in many works. Moreover, multiwavelength observations indicate an asymmetric profile that could be modeled as a jet-like feature superposed onto an expanding spherical shell. The jet-like structure can produce a γ -ray emission detectable at 100 TeV by LHAASO, CTA, and ASTRI Mini-Array [88].

2.2. Tycho SNR

Tycho's SNR is the remnant of the Type Ia SN 1572 registered by Tycho Brahe, and it has a distance of about 3 kpc. It is one of the youngest known SNRs, with an age of 450 yrs, and it is still in its ejecta-dominated phase, with a shock velocity of about 4000 km s^{-1} .

X-ray observations by the Chandra Observatory have revealed synchrotron X-ray filaments at the shock location [89] with a very high variability [90], a clear indication of the presence of an amplified magnetic field, one of the main conditions to reach VHEs.

In the γ -ray observations, there is also no clear evidence of the presence of a cutoff because the last VERITAS results have large error bars that cannot confirm it [91,92]. Its power-law spectrum, with an index $\propto E^{-2.3}$, in agreement with the theoretical expectation [93], points toward a hadronic origin of this emission.

Very recent results obtained in X-ray polarization by IXPE [94] show a dominant radial magnetic field, in agreement with the radio polarization one and the one found in CasA [95] (see Figure 4). The polarization degree is about 12%, indicating the presence of such an order in the magnetic field that, however, cannot exclude the presence of turbulence.

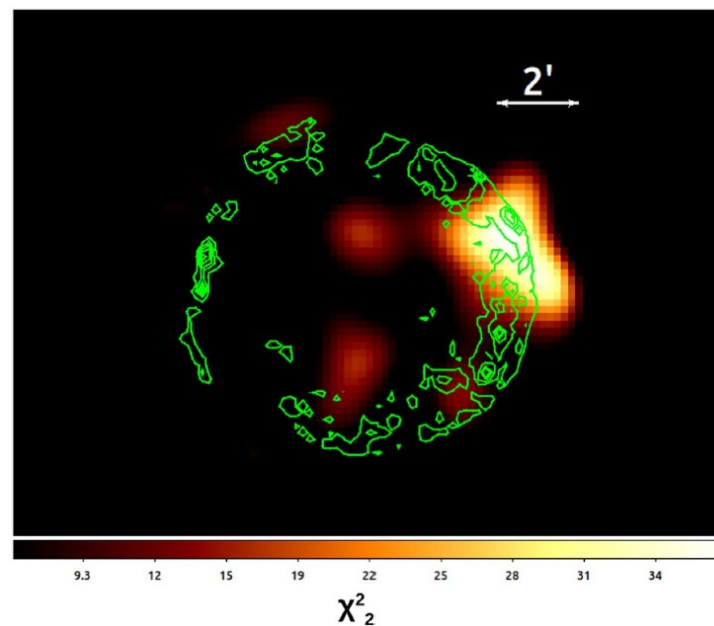


Figure 4. The polarization map of the Tycho SNR. The color scale gives the χ^2 values for the polarization signal in the 3–6 keV energy band smoothed with a Gaussian kernel. Superimposed in green are the Chandra 4–6 keV contours (figure from [94]).

These features make the Tycho SNR one of the main SNR candidate PeVatrons in the CR context and one of the best studied. However, LHAASO does not include this source in its list of candidate PeVatrons, and the most recent theoretical discussions [96,97] showed that the SNR could reach PeV energies only in the first 100 yrs of their evolution.

Only a future generation of IACTS with an effective area and a sensitivity better than those currently available will be able to better constrain the spectrum at VHEs and hence confirm or disprove the PeVatron nature of Tycho.

2.3. G 106.3+02.7

Among the first high-significance PeVatrons published by the LHAASO collaboration [15,45], there was only one source associated with an SNR: LHAASO J2226+6057, correlated with VER J2227+608/HAWC J2227+610 [98]. Its estimated age is about 10,000 years at a distance of 800 pc.

Its VHE/UHE emission could be explained by two kinds of sources: the SNR G106.3+2.7 with the associated MC in the “tail” of the TeV emission, and the Boomerang PWN, associated with the PSR J2229+6141, collocated in the “head”. The low resolution of the UHE detection by HAWC [99], Tibet ASg [100], and finally, LHAASO [45] does not allow us to say whether the γ -ray emission is from the head or the tail region.

After the second LHAASO publication [38], in which more than one SNR is a PeVatron candidate, the chance that the VHE/UHE emission comes from the SNR G106.3+2.7 is taken into account more rigorously. This remnant was discovered by the Northern Galactic plane survey in the radio band by the DRAO [101] with a comet-shaped morphology. A recent Fermi-LAT GeV analysis showed that only the tail seems to emit at the highest energies detectable by the LAT instrument (10–500 GeV), explaining the whole emission with a hadronic model from the SNR/MC interaction [102]. A hadronic origin was also declared the most likely by the MAGIC collaboration, which resolved, for the first time, the VHE/UHE emission (see Figure 5), detecting $E > 10$ TeV only from the tail region [103,104]. Several studies and analyses are ongoing to disentangle the contribution from the two possible sources (for a review, see [15]). However, the real origin of the hadronic emission will only be understood with an in-depth analysis of the microphysics of the region.

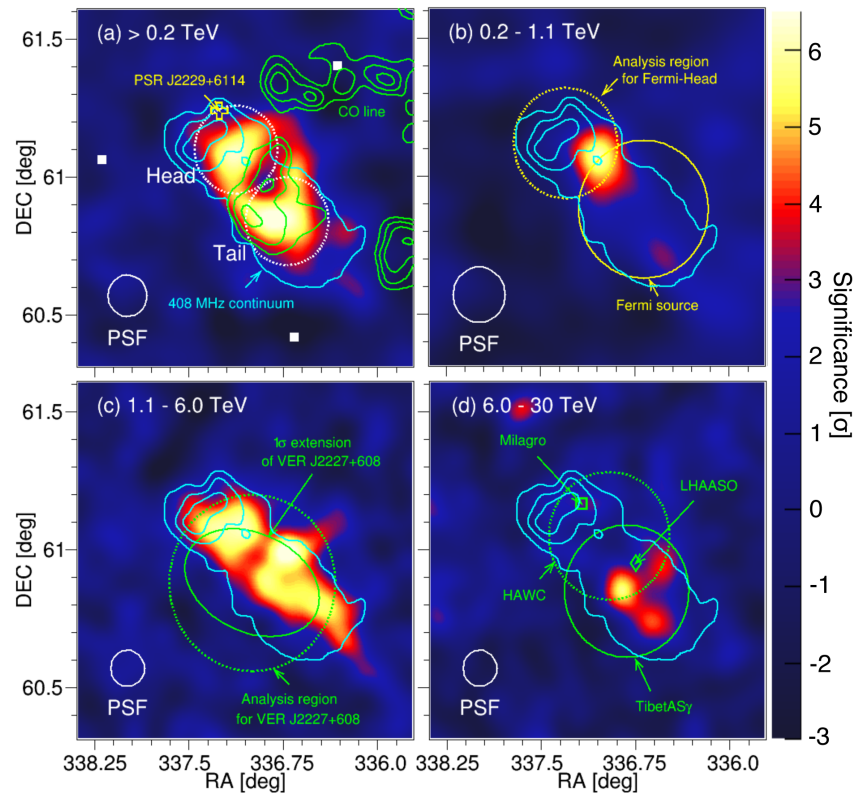


Figure 5. Energy-dependent pre-trial significance maps of the SNR G106.3+2.7 observed with the MAGIC telescopes at different energy ranges (from [104]).

In the future, the very good angular resolution of ASTRI Mini-Array [105,106] and CTA [107] could resolve the VHE emission location. Unfortunately, current estimations of the neutrino flux expected in the case of hadronic emission cannot be detected at the IceCube sensitivity [108].

2.4. RX J1713.7-3946

The “standard candle” in the debate about the hadronic or leptonic origin of the γ -ray emission from an SNR is the source RX J1713.7-3946 (G 347.3-0.5), because its GeV-TeV emission [14,69] can be reproduced with both types of models. Its age is about 1625 yrs with a distance of $d \simeq 1$ kpc [109,110] and an extension of $R_s \simeq 0.6$ deg [14].

The leptonic scenario is supported by the lack of thermal X-ray emission [111,112] and by the very good correlation between its X-ray shell [113,114] and TeV γ -ray emission. The very hard spectrum at GeV energy detected by Fermi-LAT [69] seemed a clear indication of an Inverse Compton-dominant emission (see Figure 6).

However, a more in-depth analysis of the environment in which the SNR is expanding stressed its non-homogeneous nature [115], particularly the presence of dense cloud cores in the northwestern part of the remnant, where there is enhanced X-ray emission. This could be a hint of the presence of an amplified magnetic field due to a shock–cloud interaction. The clumpy nature of the RX J1713.7-3946 environment was taken into account to explain the source γ -ray spectrum with a hadronic scenario [116–120].

For this ambiguity, RX J1713.7-3946 is the perfect candidate for the search for neutrino emission [121–123]. Indeed, after the recent results of LHAASO, it is now certain that the only way we have to finally distinguish hadronic from leptonic γ -ray emission is the detection of neutrinos correlated with VHE γ -ray.

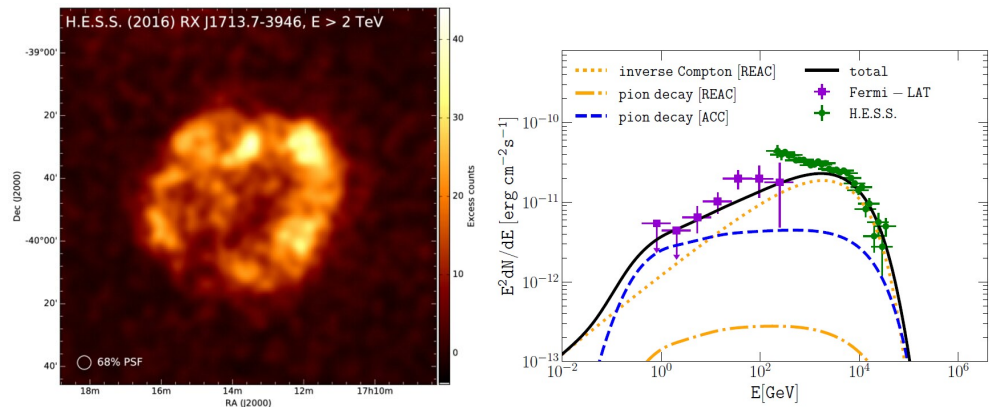


Figure 6. **Left**—The recent H.E.S.S. map of RXJ1713.7-3946, a glowing shell of γ -ray emission coincident with the outer shock of the SNR (from [124]). **Right**—The differential spectrum of the source obtained with H.E.S.S. and Fermi-LAT observations. The dotted (yellow) and dot-dashed (yellow) lines correspond to the gamma rays from re-accelerated electrons and protons. The dashed blue line corresponds to freshly accelerated protons. The solid black line is the sum of gamma rays from freshly accelerated protons and re-accelerated electrons (from [120]).

2.5. IC 443

IC 443 is a middle-aged SNR (the age is thought to be about 30,000 yr [125]) that belongs to the class of interacting SNRs; a system of MCs surrounds it [126].

In correspondence to the SNR-MC interaction region, γ -ray emission was detected in the TeV band by MAGIC [127] and VERITAS [55] and in the GeV band by AGILE [54] and Fermi [128] (see Figure 7). The association between γ -ray emission and MCs and the spectral features typical of pion decays indicate its hadronic origin [129].

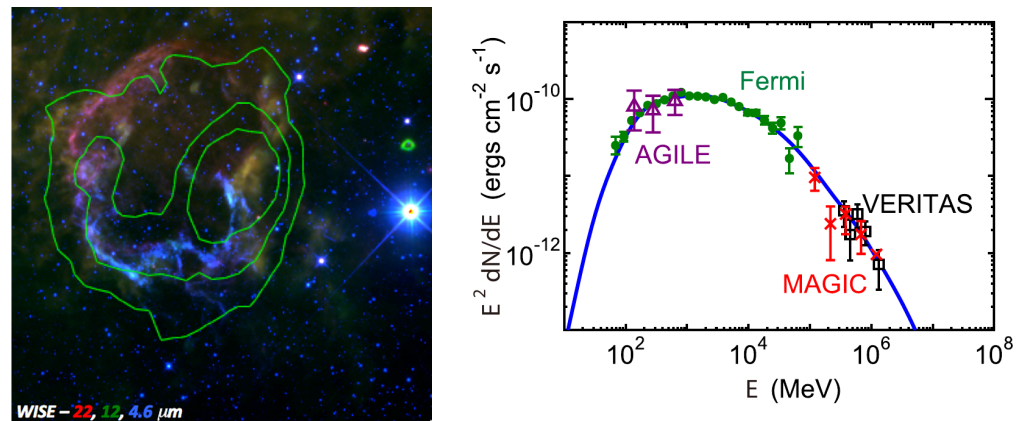


Figure 7. Morphology and spectrum of IC 443 (from [130]).

In the work in [131], an H+3 column density near IC 443 was measured, and a high ionization rate of $2 \times 10^{15} \text{ s}^{-1}$, five times larger than the typical galactic values, was found. A bright blob-like enhancement of the Fe I $K\alpha$ line located in the northwest and at the center of IC 443 was discovered [24], likely due to low-energy CR protons accelerated in the SNR leaking into the MCs and ionizing the Fe atoms therein.

A mass of about $1100 M_{\odot}$ for the ambient gas in the $[6.5, 1.5] \text{ km s}^{-1}$ range was estimated. This estimation depends on the adopted $^{12}\text{CO}/^{13}\text{CO}$ isotopic ratio. Still, it is established that a total molecular mass of $0.9\text{--}3.1 \times 10^3 M_{\odot}$ is available to interact with CRs via pion decay in a more extended region.

2.6. W 44

W44 is an interacting SNR lying at a distance of $\sim 3 \text{ kpc}$ with an estimated age of $\sim 20,000$ years. Close to the remnant, there is a giant MC; the SNR-MC interaction is

shown by the observation of OH maser emissions and a high $^{12}\text{CO}(J = 2-1)$ -to- $^{12}\text{CO}(J = 1-0)$ ratio [132]. In the radio wavelength, W 44 appears as a bright source that extends tens of arcmins. The radio spectrum is a featureless power law in the range 0.02–10.7 GHz, with evidence of spectral variations across the shell [133,134] and with no evident polarization [135]. In X-ray, this SNR is filled with thermal emission, indicating the presence of ionized gas [136].

In the GeV band, W 44 is one of the brightest sources in the sky. The link between the γ -ray emission and the SNR was proposed, for the first time, in the work in [137] on the basis of EGRET data.

It was the first SNR in whose spectrum AGILE [33,138] and Fermi [129] detected a pion bump (see Figure 8). Beyond a few GeV, the spectrum becomes very soft. Moreover, Fermi-LAT has identified two hot spots outside the SNR, aligned with it. These hot spots are believed to be the result of the anisotropic diffusion of CRs from the SNR, taking the form of CR clouds [139,140].

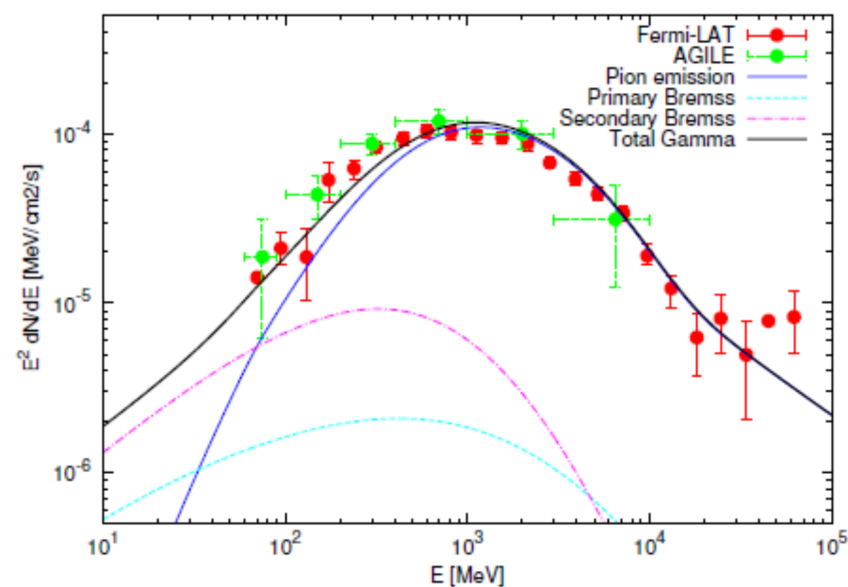


Figure 8. Gamma-ray spectrum of SNR W44 as seen by AGILE and Fermi. Hadronic and leptonic components are indicated.

2.7. Gamma Cygni

The SNR Gamma Cygni is an SNR in the constellation of Cygnus; it has an age of about 11,000 years and is characterized by a mixed morphology (a combination of a shell-like structure and a centrally filled interior) and a possible interaction with MCs. The γ -ray spectrum has been observed from a few tens of MeV to hundreds of TeV by AGILE [141], Fermi-LAT, Veritas [142], MAGIC [143] (see Figure 9), HAWC [144], and LHAASO [38].

The spectrum seems to classify this source as an interacting type of SNR. The target of the accelerated protons would be given by the gas contained in the associated MCs. These are observed in the radio band with a characteristic speed of 40–50 km s^{-1} and collect a mass of approximately $10^4 M_{\odot}$. The recent LHAASO observation of emission up to energies of about 300 TeV makes this object interesting for understanding the ability of an SNR to accelerate particles up to VHEs.

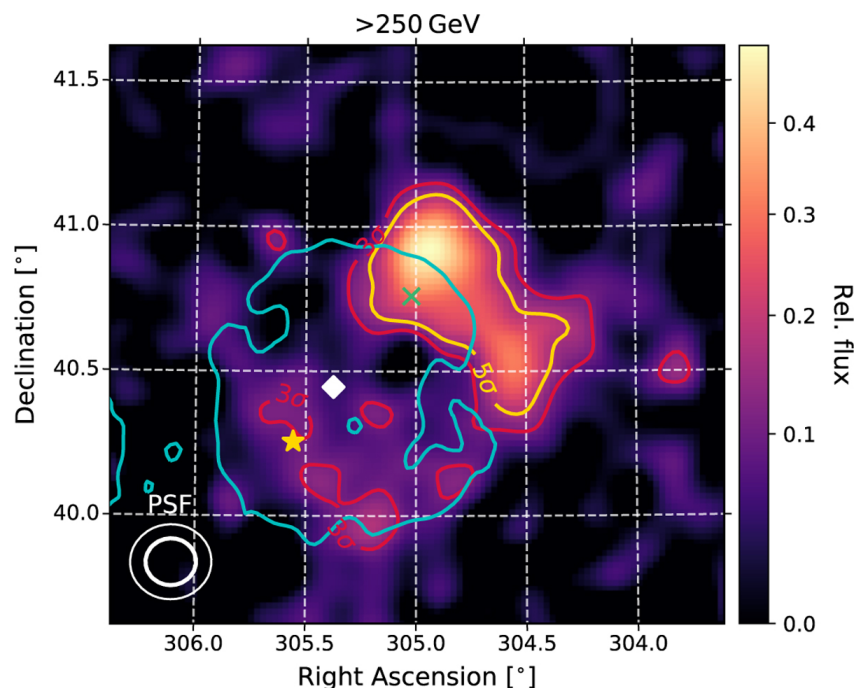


Figure 9. Gamma Cygni as seen by MAGIC [143]. The color map indicates the gamma-ray emission, while the radio shell is shown by the blue contour.

2.8. W 28

W 28 is an SNR that provides a unique opportunity to investigate the diffusion of CRs in an astrophysical environment. It is approximately 30,000 years old and lies at an estimated distance between 2 and 3.5 kpc. In continuous radio, it has a crescent shape, and the non-thermal spectrum indicates the presence of relativistic electrons in the shell [145]. W 28 provides a unique opportunity to investigate the diffusion of CRs in an astrophysical environment. Indeed, two giant MCs with masses of a few $10^4 M_{\odot}$ appear near the SNR at compatible distances [146]. One cloud partially overlaps with the SNR shell, while the other is located approximately 0.5 degrees away from the shell. The system can be modeled as having one cloud in direct contact with the SNR shock and another cloud about 10–15 parsecs away, assuming that the three objects are at the same distance and interacting with each other. Evidence of an SNR-MC system interaction comes from observations of maser emission and high ionization levels [147].

W 28 was one of the first SNRs to be indicated as a γ -ray source in the Cos B data [148]. H.E.S.S. [28], AGILE [27], and Fermi-LAT [149] observations of this object measured a γ -ray spectrum that is typical of an interacting SNR, namely, a peak below 1 GeV and a very soft spectrum above it. It is interesting to note that the peak of the γ -ray spectrum in the cloud in direct contact with the shell is at different energies than the one estimated from the other clouds. This suggests that diffusion can have an important role in this system.

3. Conclusions

For the past fifty years, SNRs have been one of the main targets of γ -ray missions. Today, about thirty SNRs have been observed with certainty in γ -rays by satellites in the GeV band, by Cherenkov telescopes in the TeV band, and more recently, by hybrid detectors like LHAASO and HAWC in the PeV band. Their study has provided answers but also raised questions. For instance, their ability to accelerate CRs (electrons and hadrons) has been demonstrated. At the same time, their spectra and morphologies have proved to be non-trivial to interpret. Another open question concerns the maximum energy at which SNRs can accelerate particles. Some of these objects have an observed spectrum that extends beyond 100 TeV, confirming that these objects may be capable of accelerating particles up to about 1 PeV. However, they represent a small minority of both the LHAASO

sources and the SNRs observed in the γ -ray regime. Overall, after almost half a century of study, it is still unclear whether or not their contribution to galactic CR acceleration is dominant compared to other sources. To answer these questions, a new generation of γ -ray instruments will come into operation in the next few years, in particular, instruments such as ASTRI Mini-Array and CTA, which will make it possible to better interpret the VHE/UHE observations that LHAASO, HAWC, and then the future SWGO will make of these objects and will finally allow us to know which astrophysical system supplies the Galaxy with its CR population.

Author Contributions: Conceptualization, A.G.; resources, M.C. and A.G.; writing—original draft preparation, A.G.; writing—review and editing, M.C. and A.G. All authors have read and agreed to the published version of the manuscript.

Funding: This research received no external funding.

Acknowledgments: We are grateful to the reviewers for their useful comments, which have enhanced the quality of our review. This research has made use of the TeVCat online source catalog (<http://tevcat.uchicago.edu>) and the SNRcat online catalog (<http://snrcat.physics.umanitoba.ca>), both accessed on 1 January 2024.

Conflicts of Interest: The authors declare no conflicts of interest.

Abbreviations

The following abbreviations are used in this manuscript:

ALPs	Axion-like particles
AS- γ	Air shower γ -ray array
ASTRI	Astrofisica con Specchi a Tecnologia Replicante Italiana
C.L.	Confidence Limit
CTAO	Čerenkov Telescope Array Observatory
DM	Dark matter
EAS	Extended air shower arrays
ESA	European Space Agency
EBL	Extra-galactic background light
E-HBL	Extreme high-peaked BL Lacs
eROSITA	Extended Roentgen survey with an imaging telescope array
FOV	Field of view
FR	Fanaroff–Riley galaxies
FSRQ	Flat-spectrum radio quasar
GASP	GLAST-AGILE Support Programme
GRB	Gamma-ray burst
GW	Gravitational wave
HAWC	High-Altitude Water Čerenkov Observatory
HB	Hadron Beam
HBL	High-peaked BL Lacs
HE	High energy
H.E.S.S.	High-Energy Stereoscopic System
IAC	Instituto de Astrofísica de Canarias
IACT	Imaging Atmospheric Čerenkov Telescope arrays
IBL	Intermediate-peaked BL Lacs
IGMF	Inter-galactic magnetic field
IR	Infra-red
IXPE	Imaging X-ray Polarimetry Explorer
LHAASO	Large High-Altitude Air Shower Observatory
LIV	Lorentz invariance violation

LST	Large-sized telescope
MAGIC	Major Atmospheric Gamma-Ray Imaging Čerenkov telescopes
MST	Medium-sized telescope
NASA	National Aeronautics and Space Administration
SBG	Star-bursting galaxies
SC	Schwarzschild–Couder
SII	Stellar intensity interferometry
SRT	Sardinia radio telescope
SST	Small-sized telescope
TNG	Telescopio Nazionale Galileo
VERITAS	Very Energetic Radiation Imaging Telescope Array System
VHE	Very high energy
WEBT	Whole-Earth Blazar Telescope

References

1. Sedov, L. *Similarity and Dimensional Methods in Mechanics*; Academic Press: Cambridge, MA, USA, 1959. [\[CrossRef\]](#)
2. Koo, B.C.; Kim, C.G.; Park, S.; Ostriker, E.C. Radiative Supernova Remnants and Supernova Feedback. *Astrophys. J.* **2020**, *905*, 35. [\[CrossRef\]](#)
3. Lee, J.J.; Park, S.; Hughes, J.P.; Slane, P.O. X-ray Observation of the Shocked Red Supergiant Wind of Cassiopeia A. *Astrophys. J.* **2014**, *789*, 7. [\[CrossRef\]](#)
4. Bell, A.R. The acceleration of cosmic rays in shock fronts—II. *Mon. Not. R. Astron. Soc.* **1978**, *182*, 443–455. [\[CrossRef\]](#)
5. Blandford, R.D.; Ostriker, J.P. Particle acceleration by astrophysical shocks. *Astrophys. J. Lett.* **1978**, *221*, L29–L32. [\[CrossRef\]](#)
6. Fermi, E. On the Origin of the Cosmic Radiation. *Phys. Rev.* **1949**, *75*, 1169–1174. [\[CrossRef\]](#)
7. Blasi, P. The origin of galactic cosmic rays. *Astron. Astrophys. Rev.* **2013**, *21*, 70. [\[CrossRef\]](#)
8. Huang, Y.; Li, Z.; Wang, W.; Zhao, X. Secondary-electron radiation accompanying hadronic GeV–TeV gamma-rays from supernova remnants. *Mon. Not. R. Astron. Soc.* **2020**, *492*, 4246–4253. [\[CrossRef\]](#)
9. Ginzburg, V.L.; Syrovatskii, S.I. *The Origin of Cosmic Rays*; Macmillan: New York, NY, USA, 1964.
10. Koyama, K.; Petre, R.; Gotthelf, E.V.; Hwang, U.; Matsuura, M.; Ozaki, M.; Holt, S.S. Evidence for shock acceleration of high-energy electrons in the supernova remnant SN1006. *Nature* **1995**, *378*, 255–258. [\[CrossRef\]](#)
11. Uchiyama, Y.; Aharonian, F.A.; Tanaka, T.; Takahashi, T.; Maeda, Y. Extremely fast acceleration of cosmic rays in a supernova remnant. *Nature* **2007**, *449*, 576–578. [\[CrossRef\]](#)
12. Vink, J. Supernova remnants: The X-ray perspective. *Astron. Astrophys. Rev.* **2012**, *20*, 49. [\[CrossRef\]](#)
13. Morlino, G.; Bandiera, R.; Blasi, P.; Amato, E. Collisionless Shocks in a Partially Ionized Medium. II. Balmer Emission. *Astrophys. J.* **2012**, *760*, 137. [\[CrossRef\]](#)
14. H. E. S. S. Collaboration; Abdalla, H.; Abramowski, A.; Aharonian, F.; Ait Benkhali, F.; Akhperjanian, A.G.; Andersson, T.; Angüner, E.O.; Arrieta, M.; Aubert, P.; et al. H.E.S.S. observations of RX J1713.7-3946 with improved angular and spectral resolution: Evidence for gamma-ray emission extending beyond the X-ray emitting shell. *Astron. Astrophys.* **2018**, *612*, A6. [\[CrossRef\]](#)
15. Cardillo, M.; Giuliani, A. The LHAASO PeVatron bright sky: What we learned. *Appl. Sci.* **2023**, *13*, 6433. [\[CrossRef\]](#)
16. Anchordoqui, L.A.; Barger, V.; Cholis, I.; Goldberg, H.; Hooper, D.; Kusenko, A.; Learned, J.G.; Marfatia, D.; Pakvasa, S.; Paul, T.C.; et al. Cosmic neutrino pevatrons: A brand new pathway to astronomy, astrophysics, and particle physics. *J. High Energy Astrophys.* **2014**, *1*, 1–30. [\[CrossRef\]](#)
17. Celli, S.; Aharonian, F.; Gabici, S. Spectral Signatures of PeVatrons. *Astrophys. J.* **2020**, *903*, 61. [\[CrossRef\]](#)
18. Funk, S. High-Energy Gamma Rays from Supernova Remnants. In *Handbook of Supernovae*; Alsabti, A.W., Murdin, P., Eds.; Springer: Cham, Switzerland, 2017; p. 1737. [\[CrossRef\]](#)
19. Acero, F.; Lemoine-Goumard, M.; Renaud, M.; Ballet, J.; Hewitt, J.W.; Rousseau, R.; Tanaka, T. Study of TeV shell supernova remnants at gamma-ray energies. *Astron. Astrophys.* **2015**, *580*, A74. [\[CrossRef\]](#)
20. Fukui, Y. Molecular and Atomic Gas in the Young TeV γ -Ray SNRs RX J1713.7-3946 and RX J0852.0-4622; Evidence for the Hadronic Production of γ -Rays. In *Cosmic Rays in Star-Forming Environments*; Torres, D.F., Reimer, O., Eds.; Astrophysics and Space Science Proceedings; Springer: Berlin/Heidelberg, Germany, 2013; Volume 34, p. 249. [\[CrossRef\]](#)
21. Jiang, B.; Chen, Y.; Wang, J.; Su, Y.; Zhou, X.; Safi-Harb, S.; DeLaney, T. Cavity of Molecular Gas Associated with Supernova Remnant 3C 397. *Astrophys. J.* **2010**, *712*, 1147–1156. [\[CrossRef\]](#)
22. Zirakashvili, V.N.; Ptuskin, V.S. Cosmic Rays and Nonthermal Radiation in Middle-Aged Supernova Remnants. *Astron. Lett.* **2018**, *44*, 769–776. [\[CrossRef\]](#)
23. Slane, P.; Bykov, A.; Ellison, D.C.; Dubner, G.; Castro, D. Supernova Remnants Interacting with Molecular Clouds: X-ray and Gamma-Ray Signatures. In *Multi-Scale Structure Formation and Dynamics in Cosmic Plasmas*; Balogh, A., Bykov, A., Eastwood, J., Kaastra, J., Eds.; Springer: Berlin/Heidelberg, Germany, 2016; Volume 51, p. 187. [\[CrossRef\]](#)

24. Nobukawa, K.K.; Nobukawa, M.; Koyama, K.; Yamauchi, S.; Uchiyama, H.; Okon, H.; Tanaka, T.; Uchida, H.; Tsuru, T.G. Evidence for a Neutral Iron Line Generated by MeV Protons from Supernova Remnants Interacting with Molecular Clouds. *Astrophys. J.* **2018**, *854*, 87. [[CrossRef](#)]
25. Acero, F.; Lemoine-Goumard, M.; Ballet, J. Characterization of the Gamma-ray Emission from the Kepler Supernova Remnant with Fermi-LAT. *Astron. Astrophys.* **2022**, *660*, A129. [[CrossRef](#)]
26. H. E. S. S. Collaboration; Aharonian, F.; Ait Benkhali, F.; Angüner, E.O.; Ashkar, H.; Backes, M.; Barbosa Martins, V.; Batzofin, R.; Becherini, Y.; Berge, D.; et al. Evidence for γ -ray emission from the remnant of Kepler's supernova based on deep H.E.S.S. observations (Corrigendum). *Astron. Astrophys.* **2024**, *683*, C1. [[CrossRef](#)]
27. Giuliani, A.; Tavani, M.; Bulgarelli, A.; Striani, E.; Sabatini, S.; Cardillo, M.; Fukui, Y.; Kawamura, A.; Ohama, A.; Furukawa, N.; et al. AGILE detection of GeV γ -ray emission from the SNR W28. *Astron. Astrophys.* **2010**, *516*, L11. [[CrossRef](#)]
28. Aharonian, F.; Akhperjanian, A.G.; Bazer-Bachi, A.R.; Behera, B.; Beilicke, M.; Benbow, W.; Berge, D.; Bernlöhr, K.; Boisson, C.; Bolz, O.; et al. Discovery of very high energy gamma-ray emission coincident with molecular clouds in the W 28 (G6.4-0.1) field. *Astron. Astrophys.* **2008**, *481*, 401–410. [[CrossRef](#)]
29. Ajello, M.; Allafort, A.; Baldini, L.; Ballet, J.; Barbiellini, G.; Bastieri, D.; Bechtol, K.; Bellazzini, R.; Berenji, B.; Blandford, R.D.; et al. Fermi Large Area Telescope Observations of the Supernova Remnant G8.7-0.1. *Astrophys. J.* **2012**, *744*, 80. [[CrossRef](#)]
30. Acero, F.; Ackermann, M.; Ajello, M.; Baldini, L.; Ballet, J.; Barbiellini, G.; Bastieri, D.; Bellazzini, R.; Bissaldi, E.; Blandford, R.D.; et al. The First Fermi LAT Supernova Remnant Catalog. *Astrophys. J. Suppl. Ser.* **2016**, *224*, 8. [[CrossRef](#)]
31. H. E. S. S. Collaboration; Abramowski, A.; Aharonian, F.; Ait Benkhali, F.; Akhperjanian, A.G.; Angüner, E.; Anton, G.; Backes, M.; Balenderan, S.; Balzer, A.; et al. Probing the gamma-ray emission from HESS J1834-087 using H.E.S.S. and Fermi LAT observations. *Astron. Astrophys.* **2015**, *574*, A27. [[CrossRef](#)]
32. MAGIC Collaboration; Acciari, V.A.; Ansoldi, S.; Antonelli, L.A.; Arbet Engels, A.; Arcaro, C.; Baack, D.; Babić, A.; Banerjee, B.; Bangale, P.; et al. Discovery of TeV γ -ray emission from the neighbourhood of the supernova remnant G24.7+0.6 by MAGIC. *Mon. Not. R. Astron. Soc.* **2019**, *483*, 4578–4585. [[CrossRef](#)]
33. Giuliani, A.; Cardillo, M.; Tavani, M.; Fukui, Y.; Yoshiike, S.; Torii, K.; Dubner, G.; Castelletti, G.; Barbiellini, G.; Bulgarelli, A.; et al. Neutral Pion Emission from Accelerated Protons in the Supernova Remnant W44. *Astrophys. J. Lett.* **2011**, *742*, L30. [[CrossRef](#)]
34. Abdo, A.A.; Ackermann, M.; Ajello, M.; Baldini, L.; Ballet, J.; Barbiellini, G.; Bastieri, D.; Bechtol, K.; Bellazzini, R.; Bloom, E.D.; et al. Fermi-LAT Study of Gamma-ray Emission in the Direction of Supernova Remnant W49B. *Astrophys. J.* **2010**, *722*, 1303–1311. [[CrossRef](#)]
35. Brun, F.; de Naurois, M.; Hofmann, W.; Carrigan, S.; Djannati-Ataï, A.; Ohm, S.; H. E. S. S. Collaboration. Discovery of VHE gamma-ray emission from the W49 region with H.E.S.S. In Proceedings of the 25th Texas Symposium on Relativistic Astrophysics, Heidelberg, Germany, 6–10 December 2010; Rieger, F.M., van Eldik, C., Hofmann, W., Eds.; p. 201. [[CrossRef](#)]
36. Abdo, A.A.; Ackermann, M.; Ajello, M.; Baldini, L.; Ballet, J.; Barbiellini, G.; Baring, M.G.; Bastieri, D.; Baughman, B.M.; Bechtol, K.; et al. Fermi LAT Discovery of Extended Gamma-Ray Emission in the Direction of Supernova Remnant W51C. *Astrophys. J. Lett.* **2009**, *706*, L1–L6. [[CrossRef](#)]
37. Aleksić, J.; Alvarez, E.A.; Antonelli, L.A.; Antoranz, P.; Asensio, M.; Backes, M.; Barres de Almeida, U.; Barrio, J.A.; Bastieri, D.; Becerra González, J.; et al. Morphological and spectral properties of the W51 region measured with the MAGIC telescopes. *Astron. Astrophys.* **2012**, *541*, A13. [[CrossRef](#)]
38. Cao, Z.; Aharonian, F.; An, Q.; Axikegu, Bai, Y.X.; Bao, Y.W.; Bastieri, D.; Bi, X.J.; Bi, Y.J.; Cai, J.T.; et al. The First LHAASO Catalog of Gamma-Ray Sources. *Astrophys. J. Suppl. Ser.* **2024**, *271*, 25. [[CrossRef](#)]
39. Katagiri, H.; Tibaldo, L.; Ballet, J.; Giordano, F.; Grenier, I.A.; Porter, T.A.; Roth, M.; Tibolla, O.; Uchiyama, Y.; Yamazaki, R. Fermi Large Area Telescope Observations of the Cygnus Loop Supernova Remnant. *Astrophys. J.* **2011**, *741*, 44. [[CrossRef](#)]
40. Lande, J.; Ackermann, M.; Allafort, A.; Ballet, J.; Bechtol, K.; Burnett, T.H.; Cohen-Tanugi, J.; Drlica-Wagner, A.; Funk, S.; Giordano, F.; et al. Search for Spatially Extended Fermi Large Area Telescope Sources Using Two Years of Data. *Astrophys. J.* **2012**, *756*, 5. [[CrossRef](#)]
41. Aliu, E.; Archambault, S.; Arlen, T.; Aune, T.; Beilicke, M.; Benbow, W.; Bird, R.; Bouvier, A.; Bradbury, S.M.; Buckley, J.H.; et al. Discovery of TeV Gamma-Ray Emission toward Supernova Remnant SNR G78.2+2.1. *Astrophys. J.* **2013**, *770*, 93. [[CrossRef](#)]
42. Pivato, G.; Hewitt, J.W.; Tibaldo, L.; Acero, F.; Ballet, J.; Brandt, T.J.; de Palma, F.; Giordano, F.; Janssen, G.H.; Jóhannesson, G.; et al. Fermi LAT and WMAP Observations of the Supernova Remnant HB 21. *Astrophys. J.* **2013**, *779*, 179. [[CrossRef](#)]
43. Xin, Y.; Zeng, H.; Liu, S.; Fan, Y.; Wei, D. VER J2227+608: A Hadronic PeVatron Pulsar Wind Nebula? *Astrophys. J.* **2019**, *885*, 162. [[CrossRef](#)]
44. Acciari, V.A.; Aliu, E.; Arlen, T.; Aune, T.; Bautista, M.; Beilicke, M.; Benbow, W.; Boltuch, D.; Bradbury, S.M.; Buckley, J.H.; et al. Detection of Extended VHE Gamma Ray Emission from G106.3+2.7 with Veritas. *Astrophys. J. Lett.* **2009**, *703*, L6–L9. [[CrossRef](#)]
45. Cao, Z.; Aharonian, F.A.; An, Q.; Axikegu, Bai, L.X.; Bai, Y.X.; Bao, Y.W.; Bastieri, D.; Bi, X.J.; Bi, Y.J.; et al. Ultrahigh-energy photons up to 1.4 petaelectronvolts from 12 γ -ray Galactic sources. *Nature* **2021**, *594*, 33–36. [[CrossRef](#)] [[PubMed](#)]
46. Castro, D.; Slane, P.; Ellison, D.C.; Patnaude, D.J. Fermi-LAT Observations and a Broadband Study of Supernova Remnant CTB 109. *Astrophys. J.* **2012**, *756*, 88. [[CrossRef](#)]
47. Abdo, A.A.; Ackermann, M.; Ajello, M.; Allafort, A.; Baldini, L.; Ballet, J.; Barbiellini, G.; Baring, M.G.; Bastieri, D.; Baughman, B.M.; et al. Fermi-Lat Discovery of GeV Gamma-Ray Emission from the Young Supernova Remnant Cassiopeia A. *Astrophys. J. Lett.* **2010**, *710*, L92–L97. [[CrossRef](#)]

48. Aharonian, F.; Akhperjanian, A.; Barrio, J.; Bernlöhr, K.; Börst, H.; Bojahr, H.; Bolz, O.; Contreras, J.; Cortina, J.; Denninghoff, S.; et al. Evidence for TeV gamma ray emission from Cassiopeia A. *Astron. Astrophys.* **2001**, *370*, 112–120. [[CrossRef](#)]
49. Giordano, F.; Naumann-Godo, M.; Ballet, J.; Bechtol, K.; Funk, S.; Lande, J.; Mazziotta, M.N.; Rainò, S.; Tanaka, T.; Tibolla, O.; et al. Fermi Large Area Telescope Detection of the Young Supernova Remnant Tycho. *Astrophys. J. Lett.* **2012**, *744*, L2. [[CrossRef](#)]
50. Acciari, V.A.; Aliu, E.; Arlen, T.; Aune, T.; Beilicke, M.; Benbow, W.; Bradbury, S.M.; Buckley, J.H.; Bugaev, V.; Byrum, K.; et al. Discovery of TeV Gamma-ray Emission from Tycho's Supernova Remnant. *Astrophys. J. Lett.* **2011**, *730*, L20. [[CrossRef](#)]
51. Katagiri, H.; Yoshida, K.; Ballet, J.; Grondin, M.H.; Hanabata, Y.; Hewitt, J.W.; Kubo, H.; Lemoine-Goumard, M. Fermi LAT Discovery of Extended Gamma-Ray Emissions in the Vicinity of the HB 3 Supernova Remnant. *Astrophys. J.* **2016**, *818*, 114. [[CrossRef](#)]
52. Araya, M. Fermi LAT observation of supernova remnant HB9. *Mon. Not. R. Astron. Soc.* **2014**, *444*, 860–865. [[CrossRef](#)]
53. Katsuta, J.; Uchiyama, Y.; Tanaka, T.; Tajima, H.; Bechtol, K.; Funk, S.; Lande, J.; Ballet, J.; Hanabata, Y.; Lemoine-Goumard, M.; et al. Fermi Large Area Telescope Observation of Supernova Remnant S147. *Astrophys. J.* **2012**, *752*, 135. [[CrossRef](#)]
54. Tavani, M.; Giuliani, A.; Chen, A.W.; Argan, A.; Barbiellini, G.; Bulgarelli, A.; Caraveo, P.; Cattaneo, P.W.; Cocco, V.; Contessi, T.; et al. Direct Evidence for Hadronic Cosmic-Ray Acceleration in the Supernova Remnant IC 443. *Astrophys. J. Lett.* **2010**, *710*, L151–L155. [[CrossRef](#)]
55. Acciari, V.A.; Aliu, E.; Arlen, T.; Aune, T.; Bautista, M.; Beilicke, M.; Benbow, W.; Bradbury, S.M.; Buckley, J.H.; Bugaev, V.; et al. Observation of Extended Very High Energy Emission from the Supernova Remnant IC 443 with VERITAS. *Astrophys. J. Lett.* **2009**, *698*, L133–L137. [[CrossRef](#)]
56. Liu, J.h.; Liu, B.; Yang, R.z. Diffuse gamma-ray emission around the Rosette Nebula. *Mon. Not. R. Astron. Soc.* **2023**, *526*, 175–180. [[CrossRef](#)]
57. Hewitt, J.W.; Grondin, M.H.; Lemoine-Goumard, M.; Reposeur, T.; Ballet, J.; Tanaka, T. Fermi-LAT and WMAP Observations of the Puppis A Supernova Remnant. *Astrophys. J.* **2012**, *759*, 89. [[CrossRef](#)]
58. Tanaka, T.; Allafort, A.; Ballet, J.; Funk, S.; Giordano, F.; Hewitt, J.; Lemoine-Goumard, M.; Tajima, H.; Tibolla, O.; Uchiyama, Y. Gamma-Ray Observations of the Supernova Remnant RX J0852.0-4622 with the Fermi Large Area Telescope. *Astrophys. J. Lett.* **2011**, *740*, L51. [[CrossRef](#)]
59. Aharonian, F.; Akhperjanian, A.G.; Bazer-Bachi, A.R.; Beilicke, M.; Benbow, W.; Berge, D.; Bernlöhr, K.; Boisson, C.; Bolz, O.; Borrel, V.; et al. H.E.S.S. Observations of the Supernova Remnant RX J0852.0-4622: Shell-Type Morphology and Spectrum of a Widely Extended Very High Energy Gamma-Ray Source. *Astrophys. J.* **2007**, *661*, 236–249. [[CrossRef](#)]
60. Saz Parkinson, P.M.; Xu, H.; Yu, P.L.H.; Salvetti, D.; Marelli, M.; Falcone, A.D. Classification and Ranking of Fermi LAT Gamma-ray Sources from the 3FGL Catalog using Machine Learning Techniques. *Astrophys. J.* **2016**, *820*, 8. [[CrossRef](#)]
61. Araya, M. Detection of gamma-ray emission in the region of the supernova remnants G296.5+10.0 and G166.0+4.3. *Mon. Not. R. Astron. Soc.* **2013**, *434*, 2202–2208. [[CrossRef](#)]
62. Yuan, Q.; Huang, X.; Liu, S.; Zhang, B. Fermi Large Area Telescope Detection of Supernova Remnant RCW 86. *Astrophys. J. Lett.* **2014**, *785*, L22. [[CrossRef](#)]
63. Aharonian, F.; Akhperjanian, A.G.; de Almeida, U.B.; Bazer-Bachi, A.R.; Behera, B.; Beilicke, M.; Benbow, W.; Bernlöhr, K.; Boisson, C.; Bochow, A.; et al. Discovery of Gamma-Ray Emission From the Shell-Type Supernova Remnant RCW 86 With HESS. *Astrophys. J.* **2009**, *692*, 1500–1505. [[CrossRef](#)]
64. Nolan, P.L.; Abdo, A.A.; Ackermann, M.; Ajello, M.; Allafort, A.; Antolini, E.; Atwood, W.B.; Axelsson, M.; Baldini, L.; Ballet, J.; et al. Fermi Large Area Telescope Second Source Catalog. *Astrophys. J. Suppl. Ser.* **2012**, *199*, 31. [[CrossRef](#)]
65. H. E. S. S. Collaboration; Abdalla, H.; Abramowski, A.; Aharonian, F.; Ait Benkhali, F.; Akhperjanian, A.G.; Andersson, T.; Angüner, E.O.; Arakawa, M.; Arrieta, M.; et al. A search for new supernova remnant shells in the Galactic plane with H.E.S.S. *Astron. Astrophys.* **2018**, *612*, A8. [[CrossRef](#)]
66. Devin, J.; Acero, F.; Ballet, J.; Schmid, J. Disentangling hadronic from leptonic emission in the composite SNR G326.3-1.8. *Astron. Astrophys.* **2018**, *617*, A5. [[CrossRef](#)]
67. Condon, B.; Lemoine-Goumard, M.; Acero, F.; Katagiri, H. Detection of Two TeV Shell-type Remnants at GeV Energies with FERMI LAT: HESS J1731-347 and SN 1006. *Astrophys. J.* **2017**, *851*, 100. [[CrossRef](#)]
68. Acero, F.; Aharonian, F.; Akhperjanian, A.G.; Anton, G.; Barres de Almeida, U.; Bazer-Bachi, A.R.; Becherini, Y.; Behera, B.; Beilicke, M.; Bernlöhr, K.; et al. First detection of VHE γ -rays from SN 1006 by HESS. *Astron. Astrophys.* **2010**, *516*, A62. [[CrossRef](#)]
69. Abdo, A.A.; Ackermann, M.; Ajello, M.; Allafort, A.; Baldini, L.; Ballet, J.; Barbiellini, G.; Baring, M.G.; Bastieri, D.; Bellazzini, R.; et al. Observations of the Young Supernova Remnant RX J1713.7-3946 with the Fermi Large Area Telescope. *Astrophys. J.* **2011**, *734*, 28. [[CrossRef](#)]
70. Aharonian, F.A.; Akhperjanian, A.G.; Aye, K.M.; Bazer-Bachi, A.R.; Beilicke, M.; Benbow, W.; Berge, D.; Berghaus, P.; Bernlöhr, K.; Bolz, O.; et al. High-energy particle acceleration in the shell of a supernova remnant. *Nature* **2004**, *432*, 75–77. [[CrossRef](#)] [[PubMed](#)]
71. Brandt, T.J.; Fermi-LAT Collaboration. A view of supernova remnant CTB 37A with the Fermi Gamma-ray Space Telescope. *Adv. Space Res.* **2013**, *51*, 247–252. [[CrossRef](#)]

72. Aharonian, F.; Akhperjanian, A.G.; Barres de Almeida, U.; Bazer-Bachi, A.R.; Behera, B.; Beilicke, M.; Benbow, W.; Bernlöhr, K.; Boisson, C.; Borrel, V.; et al. Discovery of a VHE gamma-ray source coincident with the supernova remnant CTB 37A. *Astron. Astrophys.* **2008**, *490*, 685–693. [[CrossRef](#)]
73. Xin, Y.L.; Liang, Y.F.; Li, X.; Yuan, Q.; Liu, S.M.; Wei, D.M. A GeV Source in the Direction of Supernova Remnant CTB 37B. *Astrophys. J.* **2016**, *817*, 64. [[CrossRef](#)]
74. Aharonian, F.; Akhperjanian, A.G.; Barres de Almeida, U.; Bazer-Bachi, A.R.; Behera, B.; Beilicke, M.; Benbow, W.; Bernlöhr, K.; Boisson, C.; Borrel, V.; et al. Chandra and HESS observations of the supernova remnant CTB 37B. *Astron. Astrophys.* **2008**, *486*, 829–836. [[CrossRef](#)]
75. Castro, D.; Slane, P. Fermi Large Area Telescope Observations of Supernova Remnants Interacting with Molecular Clouds. *Astrophys. J.* **2010**, *717*, 372–378. [[CrossRef](#)]
76. H. E. S. S. Collaboration; Abramowski, A.; Aharonian, F.; Ait Benkhali, F.; Akhperjanian, A.G.; Angüner, E.O.; Backes, M.; Balenderan, S.; Balzer, A.; Barnacka, A.; et al. H.E.S.S. detection of TeV emission from the interaction region between the supernova remnant G349.7+0.2 and a molecular cloud (Corrigendum). *Astron. Astrophys.* **2015**, *580*, C1. [[CrossRef](#)]
77. Yang, R.z.; Zhang, X.; Yuan, Q.; Liu, S. Fermi Large Area Telescope observations of the supernova remnant HESS J1731-347. *Astron. Astrophys.* **2014**, *567*, A23. [[CrossRef](#)]
78. H. E. S. S. Collaboration; Abramowski, A.; Acero, F.; Aharonian, F.; Akhperjanian, A.G.; Anton, G.; Balzer, A.; Barnacka, A.; Barres de Almeida, U.; Becherini, Y.; et al. A new SNR with TeV shell-type morphology: HESS J1731-347. *Astron. Astrophys.* **2011**, *531*, A81. [[CrossRef](#)]
79. Castro, D.; Slane, P.; Carlton, A.; Figueroa-Feliciano, E. Fermi-LAT Observations of Supernova Remnants Interacting with Molecular Clouds: W41, MSH 17-39, and G337.7-0.1. *Astrophys. J.* **2013**, *774*, 36. [[CrossRef](#)]
80. Krause, O.; Birkmann, S.M.; Usuda, T.; Hattori, T.; Goto, M.; Rieke, G.H.; Misselt, K.A. The Cassiopeia A Supernova Was of Type IIb. *Science* **2008**, *320*, 1195. [[CrossRef](#)]
81. Chevalier, R.A.; Oishi, J. Cassiopeia A and Its Clumpy Presupernova Wind. *Astrophys. J. Lett.* **2003**, *593*, L23–L26. [[CrossRef](#)]
82. Reed, J.E.; Hester, J.J.; Fabian, A.C.; Winkler, P.F. The Three-dimensional Structure of the Cassiopeia A Supernova Remnant. I. The Spherical Shell. *Astrophys. J.* **1995**, *440*, 706. [[CrossRef](#)]
83. Albert, J.; Aliu, E.; Anderhub, H.; Antoranz, P.; Armada, A.; Baixeras, C.; Barrio, J.A.; Bartko, H.; Bastieri, D.; Becker, J.K.; et al. Observation of VHE γ -rays from Cassiopeia A with the MAGIC telescope. *Astron. Astrophys.* **2007**, *474*, 937–940. [[CrossRef](#)]
84. Acciari, V.A.; Aliu, E.; Arlen, T.; Aune, T.; Bautista, M.; Beilicke, M.; Benbow, W.; Boltuch, D.; Bradbury, S.M.; Buckley, J.H.; et al. Observations of the Shell-type Supernova Remnant Cassiopeia A at TeV Energies with VERITAS. *Astrophys. J.* **2010**, *714*, 163–169. [[CrossRef](#)]
85. Abeyssekara, A.U.; Archer, A.; Benbow, W.; Bird, R.; Brose, R.; Buchovecky, M.; Buckley, J.H.; Chromey, A.J.; Cui, W.; Daniel, M.K.; et al. Evidence for Proton Acceleration up to TeV Energies Based on VERITAS and Fermi-LAT Observations of the Cas A SNR. *Astrophys. J.* **2020**, *894*, 51. [[CrossRef](#)]
86. Gotthelf, E.V.; Koralesky, B.; Rudnick, L.; Jones, T.W.; Hwang, U.; Petre, R. Chandra Detection of the Forward and Reverse Shocks in Cassiopeia A. *Astrophys. J. Lett.* **2001**, *552*, L39–L43. [[CrossRef](#)]
87. Morse, J.A.; Fesen, R.A.; Chevalier, R.A.; Borkowski, K.J.; Gerardy, C.L.; Lawrence, S.S.; van den Bergh, S. Location of the Optical Reverse Shock in the Cassiopeia A Supernova Remnant. *Astrophys. J.* **2004**, *614*, 727–736. [[CrossRef](#)]
88. Zhan, S.; Wang, W.; Mou, G.; Li, Z. An asymmetrical model for high-energy radiation of Cassiopeia A. *Mon. Not. R. Astron. Soc.* **2022**, *513*, 2471–2477. [[CrossRef](#)]
89. Hwang, U.; Decourchelle, A.; Holt, S.S.; Petre, R. Thermal and Nonthermal X-ray Emission from the Forward Shock in Tycho's Supernova Remnant. *Astrophys. J.* **2002**, *581*, 1101–1115. [[CrossRef](#)]
90. Matsuda, M.; Uchida, H.; Tanaka, T.; Yamaguchi, H.; Tsuru, T.G. Discovery of Year-scale Time Variability from Thermal X-ray Emission in Tycho's Supernova Remnant. *Astrophys. J.* **2022**, *940*, 105. [[CrossRef](#)]
91. Park, N.; VERITAS Collaboration. Study of high-energy particle acceleration in Tycho with gamma-ray observations. In Proceedings of the 34th International Cosmic Ray Conference (ICRC2015), The Hague, The Netherlands, 30 July–6 August 2015; Volume 34, p. 769. [[CrossRef](#)]
92. Archambault, S.; Archer, A.; Benbow, W.; Bird, R.; Bourbeau, E.; Buchovecky, M.; Buckley, J.H.; Bugaev, V.; Cerruti, M.; Connolly, M.P.; et al. Gamma-Ray Observations of Tycho's Supernova Remnant with VERITAS and Fermi. *Astrophys. J.* **2017**, *836*, 23. [[CrossRef](#)]
93. Morlino, G.; Caprioli, D. Strong evidence for hadron acceleration in Tycho's supernova remnant. *Astron. Astrophys.* **2012**, *538*, A81. [[CrossRef](#)]
94. Ferrazzoli, R.; Slane, P.; Prokhorov, D.; Zhou, P.; Vink, J.; Bucciantini, N.; Costa, E.; Di Lalla, N.; Di Marco, A.; Soffitta, P.; et al. X-ray Polarimetry Reveals the Magnetic-field Topology on Sub-parsec Scales in Tycho's Supernova Remnant. *Astrophys. J.* **2023**, *945*, 52. [[CrossRef](#)]
95. Vink, J.; Prokhorov, D.; Ferrazzoli, R.; Slane, P.; Zhou, P.; Asakura, K.; Baldini, L.; Bucciantini, N.; Costa, E.; Di Marco, A.; et al. X-ray Polarization Detection of Cassiopeia A with IXPE. *Astrophys. J.* **2022**, *938*, 40. [[CrossRef](#)]
96. Bell, A.R.; Schure, K.M.; Reville, B.; Giacinti, G. Cosmic-ray acceleration and escape from supernova remnants. *Mon. Not. R. Astron. Soc.* **2013**, *431*, 415–429. [[CrossRef](#)]

97. Cardillo, M.; Amato, E.; Blasi, P. On the cosmic ray spectrum from type II supernovae expanding in their red giant presupernova wind. *Astropart. Phys.* **2015**, *69*, 1–10. [[CrossRef](#)]
98. Wakely, S.P.; Horan, D. TeVCat: An online catalog for Very High Energy Gamma-Ray Astronomy. *Int. Cosm. Ray Conf.* **2008**, *3*, 1341–1344.
99. Albert, A.; Alfaro, R.; Alvarez, C.; Camacho, J.R.A.; Arteaga-Velázquez, J.C.; Arunbabu, K.P.; Avila Rojas, D.; Ayala Solares, H.A.; Baghmany, V.; Belmont-Moreno, E.; et al. HAWC J2227+610 and Its Association with G106.3+2.7, a New Potential Galactic PeVatron. *Astrophys. J. Lett.* **2020**, *896*, L29. [[CrossRef](#)]
100. Amenomori, M.; Bao, Y.W.; Bi, X.J.; Chen, D.; Chen, T.L.; Chen, W.Y.; Chen, X.; Chen, Y.; Cirennima, Cui, S.W.; et al. Gamma-Ray Observation of the Cygnus Region in the 100-TeV Energy Region. *Phys. Rev. Lett.* **2021**, *127*, 031102. [[CrossRef](#)] [[PubMed](#)]
101. Joncas, G.; Higgs, L.A. The DRAO galactic-plane survey. II. Field at $l = 105$. *Astron. Astrophys. Suppl. Ser.* **1990**, *82*, 113–144.
102. Fang, K.; Kerr, M.; Blandford, R.; Fleischhack, H.; Charles, E. Evidence for PeV Proton Acceleration from Fermi-LAT Observations of SNR G 106.3 +2.7. *Phys. Rev. Lett.* **2022**, *129*, 071101. [[CrossRef](#)]
103. MAGIC Collaboration; Acciari, V.A.; Ansoldi, S.; Antonelli, L.A.; Arbet Engels, A.; Baack, D.; Babić, A.; Banerjee, B.; Barres de Almeida, U.; Barrio, J.A.; et al. Resolving the origin of very-high-energy gamma-ray emission from the PeVatron candidate SNR G106.3+2.7 using MAGIC telescopes. In Proceedings of the 37th International Cosmic Ray Conference (ICRC2021), Online, 12–23 July 2021; Volume 395, p. 796.
104. MAGIC Collaboration; Abe, H.; Abe, S.; Acciari, V.A.; Agudo, I.; Aniello, T.; Ansoldi, S.; Antonelli, L.A.; Arbet Engels, A.; Arcaro, C.; et al. MAGIC observations provide compelling evidence of hadronic multi-TeV emission from the putative PeVatron SNR G106.3+2.7. *Astron. Astrophys.* **2023**, *671*, A12. [[CrossRef](#)]
105. Cardillo, M. The ASTRI Mini-Array: In the search for hidden Pevatrons. *arXiv* **2023**, arXiv:2302.10059.
106. Cardillo, M.; Tutone, A. G106.3+2.7: A candidate PeVatron with ASTRI Mini-Array. In Proceedings of the 38th International Cosmic Ray Conference (ICRC2023), Nagoya, Japan, 26 July–3 August 2023; p. 965. [[CrossRef](#)]
107. Verna, G.; Cassol, F.; Costantini, H.; Consortium, C. HAWC J2227+610: A potential PeVatron candidate for the CTA in the northern hemisphere. In Proceedings of the 37th International Cosmic Ray Conference, Online, 12–23 July 2021; p. 904. [[CrossRef](#)]
108. Sarmah, P.; Chakraborty, S.; Joshi, J.C. Probing LHAASO galactic PeVatrons through gamma-ray and neutrino correspondence. *Mon. Not. R. Astron. Soc.* **2023**, *521*, 1144–1151. [[CrossRef](#)]
109. Fukui, Y.; Moriguchi, Y.; Tamura, K.; Yamamoto, H.; Tawara, Y.; Mizuno, N.; Onishi, T.; Mizuno, A.; Uchiyama, Y.; Hiraga, J.; et al. Discovery of Interacting Molecular Gas toward the TeV Gamma-Ray Peak of the SNR G 347.3–0.5. *Publ. Astron. Soc. Jpn.* **2003**, *55*, L61–L64. [[CrossRef](#)]
110. Moriguchi, Y.; Tamura, K.; Tawara, Y.; Sasago, H.; Yamaoka, K.; Onishi, T.; Fukui, Y. A Detailed Study of Molecular Clouds toward the TeV Gamma-Ray Supernova Remnant G347.3–0.5. *Astrophys. J.* **2005**, *631*, 947–963. [[CrossRef](#)]
111. Ellison, D.C.; Patnaude, D.J.; Slane, P.; Raymond, J. Efficient Cosmic Ray Acceleration, Hydrodynamics, and Self-Consistent Thermal X-ray Emission Applied to Supernova Remnant RX J1713.7–3946. *Astrophys. J.* **2010**, *712*, 287–293. [[CrossRef](#)]
112. Katz, B.; Waxman, E. In which shell-type SNRs should we look for gamma-rays and neutrinos from P-P collisions? *J. Cosmol. Astropart. Phys.* **2008**, *2008*, 018. [[CrossRef](#)]
113. Slane, P.; Gaensler, B.M.; Dame, T.M.; Hughes, J.P.; Plucinsky, P.P.; Green, A. Nonthermal X-ray Emission from the Shell-Type Supernova Remnant G347.3–0.5. *Astrophys. J.* **1999**, *525*, 357–367. [[CrossRef](#)]
114. Tanaka, T.; Uchiyama, Y.; Aharonian, F.A.; Takahashi, T.; Bamba, A.; Hiraga, J.S.; Kataoka, J.; Kishishita, T.; Kokubun, M.; Mori, K.; et al. Study of Nonthermal Emission from SNR RX J1713.7–3946 with Suzaku. *Astrophys. J.* **2008**, *685*, 988–1004. [[CrossRef](#)]
115. Sano, H.; Fukuda, T.; Yoshiike, S.; Sato, J.; Horachi, H.; Kuwahara, T.; Torii, K.; Hayakawa, T.; Tanaka, T.; Matsumoto, H.; et al. A Detailed Study of Non-thermal X-ray Properties and Interstellar Gas toward the γ -Ray Supernova Remnant RX J1713.7–3946. *Astrophys. J.* **2015**, *799*, 175. [[CrossRef](#)]
116. Zirakashvili, V.N.; Aharonian, F.A. Nonthermal Radiation of Young Supernova Remnants: The Case of RX J1713.7–3946. *Astrophys. J.* **2010**, *708*, 965–980. [[CrossRef](#)]
117. Gabici, S.; Aharonian, F.A. Hadronic gamma-rays from RX J1713.7–3946? *Mon. Not. R. Astron. Soc.* **2014**, *445*, L70–L73. [[CrossRef](#)]
118. Inoue, T.; Yamazaki, R.; Inutsuka, S.i.; Fukui, Y. Toward Understanding the Cosmic-Ray Acceleration at Young Supernova Remnants Interacting with Interstellar Clouds: Possible Applications to RX J1713.7–3946. *Astrophys. J.* **2012**, *744*, 71. [[CrossRef](#)]
119. Celli, S. *Gamma-Ray and Neutrino Signatures of Galactic Cosmic-Ray Accelerators*; Springer Nature: Berlin/Heidelberg, Germany, 2019. [[CrossRef](#)]
120. Cristofari, P.; Niro, V.; Gabici, S. Gamma-rays and neutrinos from RX J1713–3946 in a lepto-hadronic scenario. *Mon. Not. R. Astron. Soc.* **2021**, *508*, 2204–2209. [[CrossRef](#)]
121. Kappes, A.; Hinton, J.; Stegmann, C.; Aharonian, F.A. Potential neutrino signals from galactic γ -ray sources. In Proceedings of the Journal of Physics Conference Series, Madison, WI, USA, 28–31 August 2006; Volume 60, pp. 243–246. [[CrossRef](#)]
122. Morlino, G.; Amato, E.; Blasi, P. Gamma-ray emission from SNR RX J1713.7–3946 and the origin of galactic cosmic rays. *Mon. Not. R. Astron. Soc.* **2009**, *392*, 240–250. [[CrossRef](#)]
123. Villante, F.L.; Vissani, F. How precisely can neutrino emission from supernova remnants be constrained by gamma ray observations? *Phys. Rev.* **2008**, *78*, 103007. [[CrossRef](#)]
124. O’C. Drury, L. Galactic Cosmic Rays—Theory and Interpretation. *arXiv* **2017**, arXiv:1708.08858.

125. Petre, R.; Szymkowiak, A.E.; Seward, F.D.; Willingale, R. A Comprehensive Study of the X-ray Structure and Spectrum of IC 443. *Astrophys. J.* **1988**, *335*, 215. [[CrossRef](#)]
126. Cornett, R.H.; Chin, G.; Knapp, G.R. Observations of CO emission from a dense cloud associated with the supernova remnant IC 443. *Astron. Astrophys.* **1977**, *54*, 889–894.
127. Albert, J.; Aliu, E.; Anderhub, H.; Antoranz, P.; Armada, A.; Baixeras, C.; Barrio, J.A.; Bartko, H.; Bastieri, D.; Becker, J.K.; et al. Discovery of Very High Energy Gamma Radiation from IC 443 with the MAGIC Telescope. *Astrophys. J. Lett.* **2007**, *664*, L87–L90. [[CrossRef](#)]
128. Abdo, A.A.; Ackermann, M.; Ajello, M.; Baldini, L.; Ballet, J.; Barbiellini, G.; Bastieri, D.; Baughman, B.M.; Bechtol, K.; Bellazzini, R.; et al. Observation of Supernova Remnant IC 443 with the Fermi Large Area Telescope. *Astrophys. J.* **2010**, *712*, 459–468. [[CrossRef](#)]
129. Ackermann, M.; Ajello, M.; Allafort, A.; Baldini, L.; Ballet, J.; Barbiellini, G.; Baring, M.G.; Bastieri, D.; Bechtol, K.; Bellazzini, R.; et al. Detection of the Characteristic Pion-Decay Signature in Supernova Remnants. *Science* **2013**, *339*, 807–811. [[CrossRef](#)] [[PubMed](#)]
130. Humensky, T.B. The TeV morphology of the interacting supernova remnant IC 443. In Proceedings of the Supernova Remnants: An Odyssey in Space after Stellar Death, Chania, Greece, 6–11 June 2016; p. 21.
131. Indriolo, N.; Blake, G.A.; Goto, M.; Usuda, T.; Oka, T.; Geballe, T.R.; Fields, B.D.; McCall, B.J. Investigating the Cosmic-ray Ionization Rate Near the Supernova Remnant IC 443 through $H^+ \gamma$ Observations. *Astrophys. J.* **2010**, *724*, 1357–1365. [[CrossRef](#)]
132. Yoshiike, S.; Fukuda, T.; Sano, H.; Ohama, A.; Moribe, N.; Torii, K.; Hayakawa, T.; Okuda, T.; Yamamoto, H.; Tajima, H.; et al. The Neutral Interstellar Gas toward SNR W44: Candidates for Target Protons in Hadronic γ -Ray Production in a Middle-aged Supernova Remnant. *Astrophys. J.* **2013**, *768*, 179. [[CrossRef](#)]
133. Egron, E.; Pellizzoni, A.; Iacolina, M.N.; Loru, S.; Marongiu, M.; Righini, S.; Cardillo, M.; Giuliani, A.; Mulas, S.; Murtas, G.; et al. Imaging of SNR IC443 and W44 with the Sardinia Radio Telescope at 1.5 and 7 GHz. *Mon. Not. R. Astron. Soc.* **2017**, *470*, 1329–1341. [[CrossRef](#)]
134. Loru, S.; Pellizzoni, A.; Egron, E.; Righini, S.; Iacolina, M.N.; Mulas, S.; Cardillo, M.; Marongiu, M.; Ricci, R.; Bachetti, M.; et al. Investigating the high-frequency spectral features of SNRs Tycho, W44, and IC443 with the Sardinia Radio Telescope. *Mon. Not. R. Astron. Soc.* **2019**, *482*, 3857–3867. [[CrossRef](#)]
135. Dokara, R.; Roy, N.; Menten, K.; Vig, S.; Dutta, P.; Beuther, H.; Pandian, J.D.; Rugel, M.; Rashid, M.; Brunthaler, A. Metrewave Galactic Plane with the uGMRT (MeGaPluG) Survey: Lessons from the pilot study. *Astron. Astrophys.* **2023**, *678*, A72. [[CrossRef](#)]
136. Okon, H.; Tanaka, T.; Uchida, H.; Yamaguchi, H.; Tsuru, T.G.; Seta, M.; Smith, R.K.; Yoshiike, S.; Orlando, S.; Bocchino, F.; et al. Deep XMM-Newton Observations Reveal the Origin of Recombining Plasma in the Supernova Remnant W44. *Astrophys. J.* **2020**, *890*, 62. [[CrossRef](#)]
137. Esposito, J.A.; Sreekumar, P.; Hunter, S.D.; Kanbach, G. EGRET observations of gamma-ray emission from supernova remnants. *Bull. Am. Astron. Soc.* **1996**, *28*, 861.
138. Cardillo, M.; Tavani, M.; Giuliani, A.; Yoshiike, S.; Sano, H.; Fukuda, T.; Fukui, Y.; Castelletti, G.; Dubner, G. The supernova remnant W44: Confirmations and challenges for cosmic-ray acceleration. *Astron. Astrophys.* **2014**, *565*, A74. [[CrossRef](#)]
139. Gabici, S.; Krause, J.; Morlino, G.; Nava, L. Acceleration of cosmic rays and gamma-ray emission from supernova remnant/molecular cloud associations. In Proceedings of the European Physical Journal Web of Conferences, SuGAR 2015 – Searching for the Sources of Galactic Cosmic Rays Geneva, Switzerland, 21–23 January 2015; Volume 105, p. 02001. [[CrossRef](#)]
140. Peron, G.; Aharonian, F.; Casanova, S.; Zanin, R.; Romoli, C. On the Gamma-Ray Emission of W44 and Its Surroundings. *Astrophys. J. Lett.* **2020**, *896*, L23. [[CrossRef](#)]
141. Piano, G.; Cardillo, M.; Pilia, M.; Trois, A.; Giuliani, A.; Bulgarelli, A.; Parmiggiani, N.; Tavani, M. AGILE Study of the Gamma-Ray Emission from the SNR G78.2+2.1 (Gamma Cygni). *Astrophys. J.* **2019**, *878*, 54. [[CrossRef](#)]
142. Abeysekara, A.U.; Archer, A.; Aune, T.; Benbow, W.; Bird, R.; Brose, R.; Buchovecky, M.; Bugaev, V.; Cui, W.; Daniel, M.K.; et al. A Very High Energy γ -Ray Survey toward the Cygnus Region of the Galaxy. *Astrophys. J.* **2018**, *861*, 134. [[CrossRef](#)]
143. MAGIC Collaboration; Acciari, V.A.; Ansoldi, S.; Antonelli, L.A.; Arbet Engels, A.; Baack, D.; Babić, A.; Banerjee, B.; Barres de Almeida, U.; Barrio, J.A.; et al. Study of the GeV to TeV morphology of the γ Cygni SNR (G 78.2+2.1) with MAGIC and Fermi-LAT. Evidence for cosmic ray escape. *Astron. Astrophys.* **2023**, *670*, A8. [[CrossRef](#)]
144. Albert, A.; Alfaro, R.; Alvarez, C.; Camacho, J.R.A.; Arteaga-Velázquez, J.C.; Arunbabu, K.P.; Avila Rojas, D.; Ayala Solares, H.A.; Baghmanyan, V.; Belmont-Moreno, E.; et al. 3HWC: The Third HAWC Catalog of Very-high-energy Gamma-Ray Sources. *Astrophys. J.* **2020**, *905*, 76. [[CrossRef](#)]
145. Dubner, G.M.; Velázquez, P.F.; Goss, W.M.; Holdaway, M.A. High-Resolution VLA Imaging of the Supernova Remnant W28 at 328 and 1415 MHz. *Astron. J.* **2000**, *120*, 1933–1945. [[CrossRef](#)]
146. Mizuno, A.; Fukui, Y. Physical properties of molecular clouds as revealed by NANTEN CO survey: From the galactic center to the galactic warp. In Proceedings of the Milky Way Surveys: The Structure and Evolution of our Galaxy, Boston, MA, USA, 15–17 June 2003; Clemens, D., Shah, R., Brainerd, T., Eds.; Astronomical Society of the Pacific Conference Series; Astronomical Society of the Pacific: San Francisco, CA, USA, 2004; Volume 317, p. 59.
147. Frail, D.A.; Goss, W.M.; Slysh, V.I. Shock-excited maser emission from the supernova remnant W28. *Astrophys. J. Lett.* **1994**, *424*, L111–L113. [[CrossRef](#)]

148. Pollock, A.M.T. The probable identification of two COS-B gamma-ray sources with molecular clouds compressed by supernova remnants. *Astron. Astrophys.* **1985**, *150*, 339–342.
149. Abdo, A.A.; Ackermann, M.; Ajello, M.; Allafort, A.; Baldini, L.; Ballet, J.; Barbiellini, G.; Bastieri, D.; Bechtol, K.; Bellazzini, R.; et al. Fermi Large Area Telescope Observations of the Supernova Remnant W28 (G6.4-0.1). *Astrophys. J.* **2010**, *718*, 348–356. [[CrossRef](#)]

Disclaimer/Publisher’s Note: The statements, opinions and data contained in all publications are solely those of the individual author(s) and contributor(s) and not of MDPI and/or the editor(s). MDPI and/or the editor(s) disclaim responsibility for any injury to people or property resulting from any ideas, methods, instructions or products referred to in the content.